Shiraz University

IJVR
ISSN: 1728-1997 (Print)
ISSN: 2252-0589 (Online)

Vol. 23 No.1 Ser. No. 78 2022

IRANIAN JOURNAL OF VETERINARY RESEARCH

Original Article

Evaluation of the properties and antibacterial activity of microchitosan film impregnated with Shirazi thyme (*Zataria multiflora*) and garlic (*Allium sativum*) essential oils

Ebadi, Z.[1]; Ghaisari, H.[2]; Tajeddin, B.[3] and Shekarforoush, S. S.[2*]

[1]Ph.D. Student in Food Hygiene, Department of Food Hygiene and Public Health, School of Veterinary Medicine, Shiraz University, Shiraz, Iran, and Animal Science Research Institute (ASRI), Agricultural Research, Education and Extension Organization (AREEO), Karaj, Iran (current address); [2]Department of Food Hygiene and Public Health, School of Veterinary Medicine, Shiraz University, Shiraz, Iran; [3]Agricultural Engineering Research Institute (AERI), Agricultural Research, Education and Extension Organization (AREEO), Karaj, Iran

[*]***Correspondence:*** *S. S. Shekarforoush, Department of Food Hygiene and Public Health, School of Veterinary Medicine, Shiraz University, Shiraz, Iran. E-mail: shekar@shirazu.ac.ir*

10.22099/IJVR.2021.38534.5609

(Received 22 Sept 2020; revised version 20 Aug 2021; accepted 6 Nov 2021)

Abstract

Background: Recent research has shown that chitosan has good moisture-absorbing properties at the micro and nanoscale, and seems to be a good candidate for the production of biodegradable moisture-absorbing films. **Aims:** The aim of this study was to evaluate the properties and antibacterial activity of starch-based microchitosan (MCH) films impregnated with two essential oils (EOs). **Methods:** MCH films with varying thicknesses were made from cornstarch (6%), microchitosan (1%), glycerol (2.25%), and/or EOs (2%), and their characteristics, including swelling degree (SD), tensile strength (TS), and elongation at break (EB%), were examined. The film structures were confirmed by X-ray diffraction (XRD), scanning electron microscopy (SEM), and atomic force microscopy (AFM). To determine the antibacterial activity against *Escherichia coli* and *Staphylococcus aureus*, two EOs of Shirazi thyme, garlic, and a mixture of them were used in the experimentation. **Results:** The EB% and TS had a linear relationship with the thickness of samples and improved by increasing the thickness of films. The XRD pattern showed that the MCH films had an amorphous structure. SEM of the films showed a homogeneous dispersion of MCH in the starch matrix without any porosity. The AFM images showed a simultaneous increase in the thickness of the MCH films and surface roughness. The film was able to absorb water up to 15.78 times its weight in 48 h. The inhibition zone of films containing 2% thyme EO was 42.0 mm for *S. aureus* and 12.3 mm for *E. coli* ($P<0.05$). **Conclusion:** MCH film containing Shirazi thyme can be described as a moisture-absorbing antibacterial pad and is a new idea for active food packaging to increase the shelf life of foods with fully degradable properties.

Key words: Anti-bacterial, Food packaging, Microchitosan, Moisture absorbent pad, Starch matrix film

Introduction

The most common food packaging materials are plastics (about 50%) (FICCI, 2016; Jeevahan and Chandrasekaran, 2019), and due to many economic and practical aspects such as low cost, light weight, and convenience, it is estimated that their use will increase in the future. Biopolymers and films have been considered by researchers as a desirable option that has a great capacity for artificial replacement. However, the film properties are not the same as traditional packaging materials, such as synthetic plastics (Turalija *et al*., 2016; Bhardwaj *et al*., 2019).

One of the main biopolymers is polysaccharides. They have many properties that make them attractive for use in the food industry, including hydrophilicity, biodegradability, biocompatibility, low toxicity, bioactivity, antimicrobial activity, thickening, and film formation (Mohamad and Fahmy, 2012; Chanphai and Tajmir-Riahi, 2018; Ribeiro *et al*., 2018). Considerable investigation has been recently directed to the use of naturally abundant polymers such as chitin, cellulose, and chitosan to produce films (Amjadi *et al*., 2019; Noorbakhsh-Soltani *et al*., 2019; Yang *et al*., 2020). Chitin and chitosan are natural amino polysaccharides that are produced in about the same amount as cellulose (Kumar, 2000). They have an exceptional performance in making bio-composites. Chitosan is a green compound generally applied in different fields, including food, agriculture, biomedicine, cosmetics, and other industries. Several reports including different attributes of the chitosan functions have been published in recent years (Kumar, 2000; Amidi *et al*., 2010; Mohamad and Fahmy, 2012; Chanphai and Tajmir-Riahi, 2018; Silva *et al*., 2018; Qin *et al*., 2019; Sun *et al*., 2019).

Chitosan is a cationic biopolymer that makes it appropriate for binding to negative-charged materials (Wei *et al*., 2009; Ribeiro *et al*., 2018). The chemical

properties of chitosan are defined by the molecular weight, degree of deacetylation, and viscosity (van der Lubben *et al*., 2001). The molecular weight of the chitosan can be low, medium, or high (70, 190-310, or 500 kDa, respectively) (Schiffman and Schauer, 2007).

The main cause of food spoilage is moisture in foods and food respiration, which affects the quality and shelf life of food products. Recently, the effective method of monitoring and binding excess water accumulations in active packaging systems, has found much interest, and moisture scavengers such as sachets, pads, or sheets have been introduced. Many moisture absorbers in markets consist of silica gel, natural clays, calcium chloride, and polymeric materials (Ozdemir and Floros, 2004; Bhardwaj *et al*., 2019). A few articles have discussed replacing natural moisture-absorbing films with synthetic ones. Natural moisture-absorbing films can be used because of their ability to overcome the problems associated with water condensation in food packaging.

Besides, many reports have shown that chitosan at micro and nano scales has moisture-absorbing and antibacterial properties (Radusin *et al*., 2016; Turalija *et al*., 2016; Qin *et al*., 2019), and the essential oils (EOs) may enhance the antimicrobial activity of films. Therefore, in this study, microchitosan (MCH) film impregnated with two EOs as a degradable moisture-absorbing antibacterial pad was prepared, and its mechanical and antibacterial properties were evaluated.

Materials and Methods

Materials

MCH (deacetylation, 85%) with the molecular weight of 50-80 KDa and mesh size 60 µm were produced in Nano Novin Polymer Co. (Sari, Mazandaran, Iran). Calcium chloride anhydrous was provided by Duksan Co., Korea. Magnesium nitrate and glycerol were purchased from Fluka Co. and Merck Co., Germany, respectively. EOs of Shirazi thyme *(Zataria multiflora*) and garlic (*Allium sativum*) were purchased from Barij Essence and Herbal Exir Companies (Iran). *Escherichia coli* (ATCC 35218) and *Staphylococcus aureus* (ATCC 6538) were provided by the Department of Food Hygiene and Public Health, School of Veterinary Medicine, Shiraz University, Iran. Corn starch containing approx. 73% amylopectin and 27% amylose was purchased from Sigma-Aldrich (S4126, EC: 232-679-6), USA.

Methods

Film preparation

The films were prepared according to Chaichi *et al*. (2017) method, with some modifications. Three grams of corn starch were dissolved in 50 ml of aqueous solution of acetic acid (1% v/v) and stirred using a stirrer heater at room temperature for 30 min at 1000 ×g (Heidolf, Standard Hei, Germany). In parallel, 1.00 g of MCH was dispersed in 40 ml of aqueous solution of acetic acid (1% v/v) and stirred at room temperature for 30 min at 1000 ×g. After complete dissolution, 2.25 g of glycerol was added. The solutions were then mixed, the volume adjusted to 100 ml with acetic acid (1% v/v), and stirred again at 90°C at 1000 ×g for 30 min. The homogenized solutions were poured into Petri dishes and permitted to dry at room temperature (3-4 days). The dried films were removed from the plates and placed in a desiccator containing a saturated magnesium nitrate solution at 25°C and 52.8% relative humidity (RH) for at least 48 h. The different thicknesses of films were attained using different amounts of (g) intended solutions in the Petri dishes.

To produce antibacterial films, 2% of Shirazi thyme and garlic EOs and a mixture of them (1% of each) and tween 80 (0.1% V/V for each percentage of EOs) were added to the final solution and homogenized using a high-shear mixing homogenizer (Heidolph-DIAX900, Germany) at 14000 ×g for 3 min. The other stages of production were the same as before.

Film characterization

Thickness

The thickness of films was measured using a digital micrometer (Mitutoyo Co., Japan), with an accuracy of 0.001 mm. Five points were randomly selected in each sample and their thickness was measured. Their mean was reported as the sample thickness.

Swelling degree (SD)

Film samples were cut into 2 × 2 cm^2 pieces; after weighting (w_i), they were immersed in distilled water, and the swelling capacities were measured at intervals of 1, 24, and 48 h. The SD of the films was calculated by the following equation (Lavorgna *et al*., 2010):

$$SD = \frac{W_f - W_i}{W_i}$$

Where,

W_f: The final weights (in g) of the samples

W_i: The initial weights (in g) of the samples

Mechanical properties

The mechanical properties of the films were measured using a texture analyzer (Hounsfield, Model H5KS, UK) with a 500 N load cell, according to ASTM standard method D882 (ASTM, 2007). Prior to the test, the films were cut into rectangular strips with a dimension of 4 × 1 cm^2. The initial grip spacing and crosshead speed were set at 40 mm and 10 mm per min, respectively. Tensile strength (TS) and the presence of elongation at break (EB%) were calculated by the following equations:

$$TS\ MPa = \frac{\text{Maximum force}}{(\text{Film thickness}) \times (\text{Film width})}$$

$$EB\% = \frac{\text{Final length} - \text{Initial length}}{\text{Initial length}} \times 100$$

X-ray diffraction (XRD)

The film samples were analyzed for XRD properties according to Koo (2019) by an X-ray Diffractometer

(Model X'Pert MPD, Panalytical, Netherlands).

Scanning electron microscopy (SEM)

A scanning electron microscope (VEGA, TESCAN, Czech Republic) was used to examine the morphology of the films. Briefly, film samples were frozen with liquid nitrogen, fractured, mounted, coated with gold (2 min) on a sputter coater (K450x-EMITECH-England), and finally observed. All SEM photomicrographs were obtained using an accelerating voltage of 10 kV and at different magnifications (1000, 5000, and ×15000).

Atomic force microscopy (AFM)

Topographical images of MCH films were performed using a multimode atomic force microscope (Dualscope/Rasterscope C26, DME, Denmark). The height (S_z), average roughness (Sa), and root mean square surface roughness (Sq) values of different scan sizes of two different film thicknesses were calculated. The equipment was operated in a non-contact mode in the air using a silicon tip (curvature radius <10 nm and a cantilever length of 230 µm) with a resonance frequency of 175 kHz.

Gas chromatography/mass spectrometry (GC/MS) analysis of EOs

GC/MS analysis was carried out using an Agilent 6890 GC/MS instrument equipped with BPX5 capillary columns (30 m × 0.25 mm i.d., 0.25 µm thickness, Agilent technologies). Helium was used as the carrier gas while the flow rate was adjusted to 1 ml/min, and an injection volume of 1 µL was used. The mass spectrometer was run in the electron ionization (EI) mode at 70 eV. The injector temperature was 220°C, and the detector temperature was 290°C. The data were collected under the following conditions: an initial temperature of 60°C, a program rate of 2°C/min for the polar column (up to 220°C), and 3°C/min for the non-polar column (up to 240°C). The ingredients of EOs were identified by comparison of their relative retention times and mass spectra with Willey7n, NIST98 (National Institute of Standards) and Adam's library spectra (Adams and Sparkman, 2007).

Antibacterial activity

The antimicrobial activity of the films was measured by the disc diffusion method. In aseptic conditions, 6 mm diameter discs were made from the films using punctures. The discs were placed on the surface of the nutrient agar plate inoculated with 0.1 ml of *S. aurous* and *E. coli* suspension (approximately containing 10^6 CFU/ml). The plates were then incubated at 37°C for 24 h. Then, the diameter of the inhibition zone around the discs was measured. Three independent replicates were carried out for each sample, with two duplicates (Jalaei *et al*., 2014).

Statistical analysis

A completely randomized design with a factorial arrangement was used for statistical analysis. Analysis of variance was performed using a general linear model (GLM) within the SAS package (SAS, 2013). Data were also analyzed by the repeated measurement method, and differences between means were tested using Duncan's new multiple range test within the SAS package (SAS, 2013).

Results

Film characterization

SD

Figure 1 depicts the SD of MCH film. The highest SD was observed in MCH samples with a thickness of 260 µm after 48 h (P<0.05). The results indicated that the SD of MCH was increased by increasing the thickness and passing the time (P<0.05). The films have not reached equilibrium swelling after 48 h.

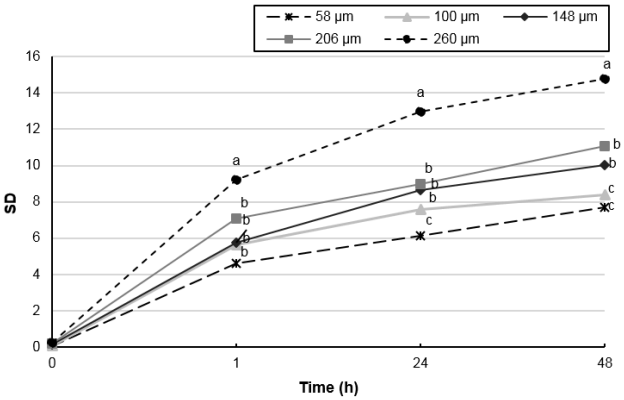

Fig. 1: Swelling degree (SD) of microchitosan (MCH) film in different thicknesses and time intervals. *: 90 µm, ▲: 125 µm, ♦: 175 µm, ■: 225 µm, and ●: 260 µm. n=3. Different letters indicate the significant difference between different thicknesses within each time (P<0.05)

Mechanical properties

The EB% and TS of MCH films are shown in Fig. 2. EB% had a linear relationship with the thickness of samples, which improved by increasing the thickness of films. The highest flexibility was observed in films with a thickness of 260 µm. The TS level of MCH with a thickness of 100-260 µm was less than 3.7 MPa, which is a conventional requirement for a food packaging material (Jeevahan and Chandrasekaran, 2019).

XRD analysis

The XRD patterns of the neat MCH and MCH films in two different thicknesses are presented in Figs. 3A-C. One peak was observed at 2θ = 20.22° in MCH films, and two sharp peaks were observed at 2θ = 10.50° and 20.22° in neat MCH. The percentage of crystallinity of neat MCH and MCH films with 125 and 175 µm thickness was 33.73, 28.25, and 23.22, respectively (Table 1).

SEM analysis

The SEM image of the surface and cross section of MCH in different thicknesses is shown in Figs. 4A-D.

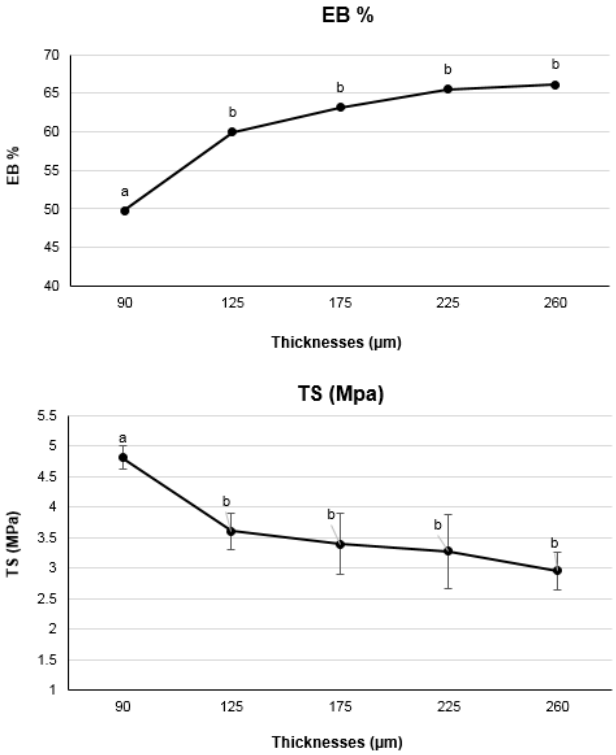

Fig. 2: Percentage of elongation at break (EB%) and tensile strength (TS) of different thicknesses of microchitosan (MCH) film. Different letters indicate the significant difference (P<0.05)

Table 1: Crystallinity percentage of neat and films of microchitosan (MCH)

Microchitosan	Sum of net area	Sum of gross area	Crystallinity %
Neat	4692.14	13910.13	33.73
Film (thickness: 125 µm)	5397.72	19106.86	28.25
Film (thickness: 175 µm)	5198.44	22390.99	23.22

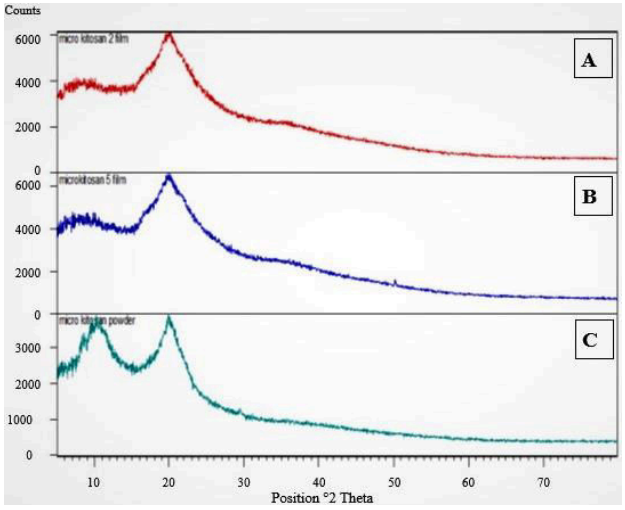

Fig. 3: The X-ray diffraction (XRD) patterns of microchitosan films in different thicknesses (**A**: 125 µm, **B**: 175 µm, and neat microchitosan (**C**))

SEM of the films showed homogeneous dispersion of MCH in the starch matrix without any porosity. However, there was slight sedimentation in the films which could be related to the micro size of MCH and the presence of starch through the drying process (Vigneshwaran *et al*., 2006; Ma *et al*., 2016).

AFM analysis

Topographical images of three different scan sizes of two different thicknesses of MCH films are shown in Fig. 5. The roughness on the film surface can affect its mechanical and physical properties. AFM images presented that the thick MCH films had the highest projections and the roughest surfaces, so the MCH films with the highest thickness had rougher surfaces (Fig. 5). Table 2 summarizes the S_z, Sq, and S_a parameters of different thicknesses of MCH in three scan sizes. As shown, the low thickness of MCH films had the lowest S_q in all scan sizes.

Table 2: Comparison of arithmetic mean of height (S_Z), roughness (S_q), and average roughness (S_a) values of different scan sizes of two different thickness microchitosan films

Thickness (µm)	Scan size (µm)	S_z (nm)	S_q (nm)	S_a (nm)
125	3 × 3	73.9	10.3	7.85
	5 × 5	138.0	14.6	10.7
	10 × 10	186.0	24.6	19.0
175	3 × 3	64.0	14.0	11.5
	5 × 5	88.5	21.4	17.3
	10 × 10	182.0	41.0	33.3

Antibacterial activity

Main components of the EOs of Shirazi thyme and garlic as identified by GC/MS analysis are shown in Table 3. Thymol (39.14%) and carvacrol (26.61%) were the main components of Shirazi thyme EO. Diallyl disulfide (20.18%) and diallyl trisulfide (32.82%) were the main components of garlic EO.

Table 3: Main components (%) of the essential oils (EOs) of Shirazi thyme (*Zataria multiflora*) and garlic (*Allium sativum*)

Compounds	Shirazi thyme	Garlic
α-Pinene	3.34	-
ρ-Cymen	7.88	-
γ-Terpinene	6.57	-
Thymol	39.14	-
Carvacrol	26.61	-
Caryophyllene	2.11	-
Allyl n-propyl sulfide	-	3.53
3-Methylthiophene	-	0.1
Allyl methyl disulfide	-	7.18
Diallyl disulfide	-	20.18
Diallyl trisulfide	-	32.82

The antimicrobial effects of Shirazi thyme and garlic EOs alone and in combination against *E. coli* and *S. aureus* were evaluated.

Table 4 shows that there were no apparent inhibition zones around samples of MCH and MCH containing garlic EO for *E. coli* and *S. aureus*, but there were apparent inhibition zones against these bacteria around the films containing EO of Shirazi thyme. The inhibition zone against *E. coli* and *S. aureus* around the film with

MCH containing EO of Shirazi thyme was much larger than that of the MCH containing both EOs. Briefly, MCH containing Shirazi thyme and Shirazi thyme + garlic EOs exhibited distinct antibacterial efficacy against *S. aureus* and *E. coli*.

Table 4: Diameter of inhibition zone (mm) against *E. coli* and *S. aureus* around the microchitosan (MCH) films containing essential oils (EOs) of Shirazi thyme and garlic

Treatment groups	Inhibition diameter (mm)	
	E. coli	*S. aureus*
Control	0.0[a]	0.0[a]
Garlic EO	0.0[a]	0.0[a]
Thyme EO	12.3 ± 0.9[b]	42.0 ± 3.1[b]
Garlic + thyme EOs	8.5 ± 0.3[c]	35.8 ± 0.6[c]

The different letters indicate significant differences among treatment groups (P<0.05)

Discussion

The samples with a thickness of 260 µm were able to absorb water more than 14 times their weight. It seems that MCH can be a suitable and notable moisture absorbent pad for food packaging.

The optimized MCH improved mechanical properties compared with some synthetic films (Jeevahan and Chandrasekaran, 2019). It seems that improvement of the mechanical and elongation at break properties for the micro film is due to the cellulosic component through interfacial hydrogen and ionic interactions (Cao *et al*., 2008). This is attributed to the good interfacial interaction between the fillers and matrix, which was an important factor affecting the mechanical properties of the composites (Ma *et al*., 2009). Consequently, a suitable and equal distribution of applied stress reduces the stress concentrations and increases the flexibility of films (Kanagaraj *et al*., 2007; Chaichi *et al*., 2017). Frone *et al*. (2013) reported that the supplement of micro-fibrillated cellulose improved the elasticity modulus of biodegradable polymers of polylactic acid (PLA) XRD patterns and the crystallinity percentage showed that the MCH was present in the films at

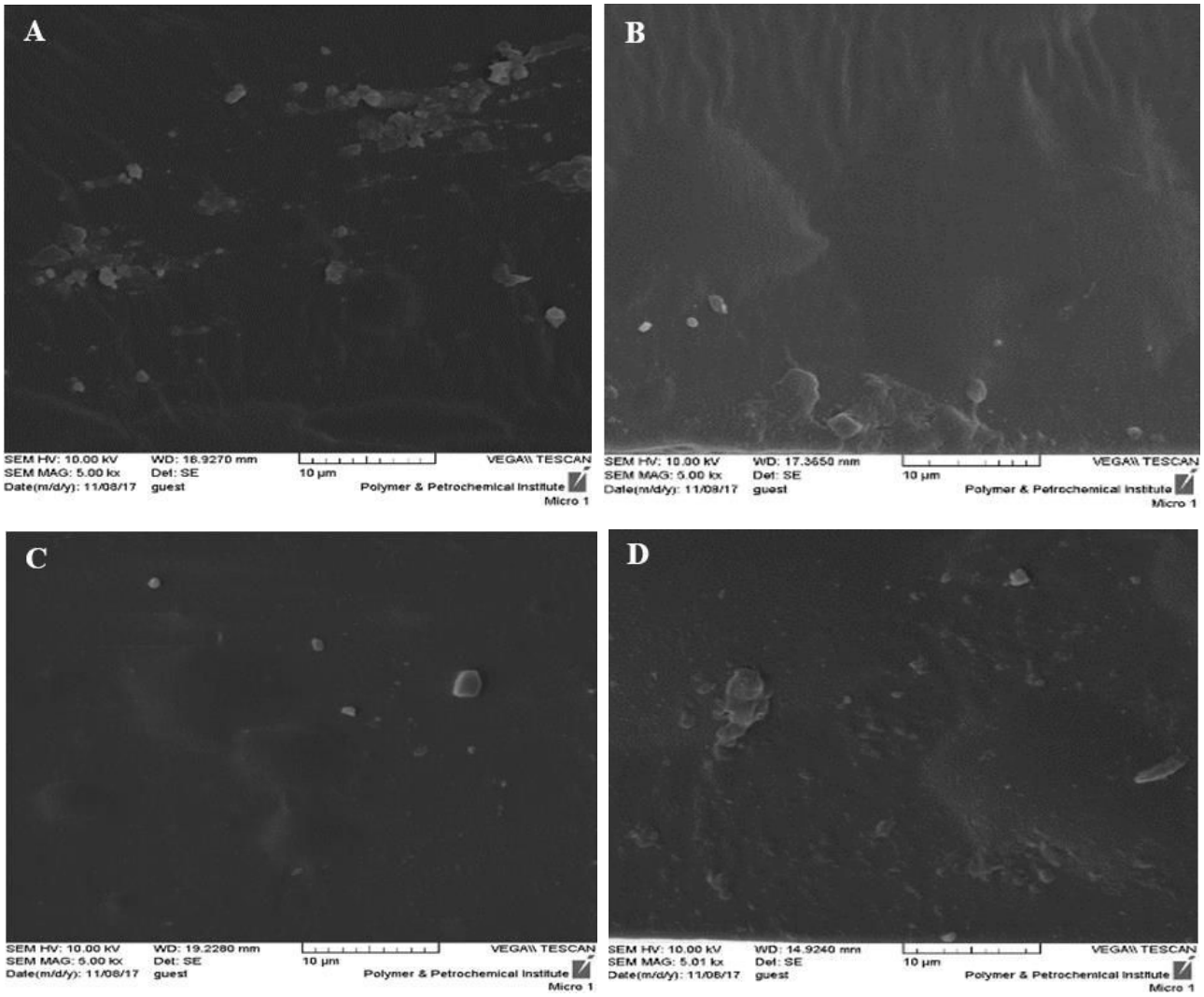

Fig. 4: Scanning electron microscope (SEM) images of the surface (**A** and **C**) and cross-section (**B** and **D**) morphology of microchitosan (MCH) film in low thickness (125 µm) and high thickness (175 µm), respectively

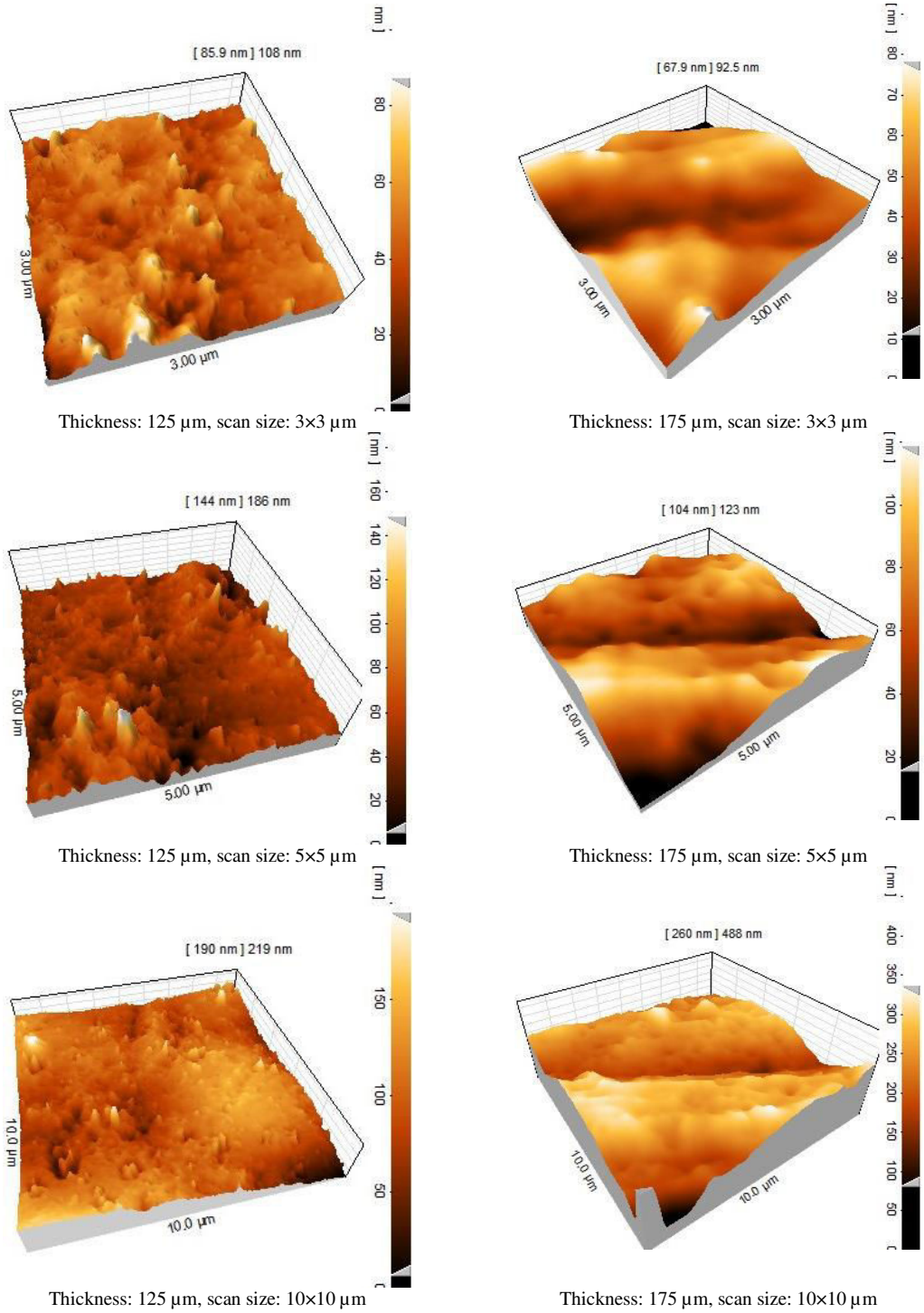

Thickness: 125 µm, scan size: 3×3 µm

Thickness: 175 µm, scan size: 3×3 µm

Thickness: 125 µm, scan size: 5×5 µm

Thickness: 175 µm, scan size: 5×5 µm

Thickness: 125 µm, scan size: 10×10 µm

Thickness: 175 µm, scan size: 10×10 µm

Fig. 5: Topographic images of MCH films in different scan sizes of two different thickness. The images were obtained using a multimode atomic force microscope

different thicknesses. Also, the crystallinity degree of neat MCH was higher than that found for MCH films, which indicated that the amorphous structure of neat MCH was lower than the MCH films. An amorphous structure could increase the amount of moisture absorption of samples. Hence, the SD levels of MCH in thick samples were higher than in thin ones (Fig. 1).

Topographical images showed suitable dispersion of MCH in the starch matrix, indicating appropriate interaction between the filler and the matrix, which is in agreement with mechanical outcomes. As seen in Fig. 5, with increasing thickness, the presence of uneven plateaus on the AFM images increased and revealed more affinity for agglomerate. These are found to validate the finding of the SEM pictures. Mandal and Chakrabarty (2015) reported that at the higher level of biopolymer integration, the elements display an extra tendency to agglomerate, thus making micro or macro composites.

Shirazi thyme belongs to the Laminaceae family that

grows in Iran, Pakistan, and Afghanistan, and this plant is widely used as a flavouring agent in several foods. Shirazi thyme has inhibitory activity on Gram-negative and Gram-positive bacteria due to having different amounts of phenolic compounds in leaves, flowers, and roots (Shirdel *et al*., 2017; Qin *et al*., 2019).

The antibacterial mechanism of garlic is due to the competitive inhibition of sulfhydryl-containing enzymes (specific inhibition of RNA synthesis and lipid biosynthesis) (Morales-González *et al*., 2019). Numerous studies have shown that garlic EO has antimicrobial effects against foodborne pathogens. Diallyl disulfide and diallyl trisulfide are the main components of garlic EO (WU *et al*., 2008), which are considered to be the main antimicrobial compounds of garlic EO (Yin and Cheng, 2003; Rattanachaikunsopon and Phumkhachorn, 2009). In the present study, a MCH film containing 2% garlic EO had no inhibitory effect on *E. coli* and *S. aureus*. In the study by Seydim and Sarikus (2006), a concentration of 2% of this EO along with whey protein-based edible films had no inhibitory effect against foodborne bacteria.

In the presence of EO of Shirazi thyme, the Gram-negative bacterial strains of *E. coli* had smaller inhibition zones than those of Gram-positive bacterial strains of *S. aureus*. This indicated that the *E. coli* strain exhibited higher resistance to Shirazi thyme than the *S. aureus* strain. The present results are consistent with the results that have worked on the antibacterial effects of films containing garlic and Shirazi thyme by many researchers (Rahimi *et al*., 2019; Qin *et al*., 2019).

This study prepared a starch-based film from MCH as a moisture-absorbing pad. The film had a considerable water absorption capacity, which increased with increasing the thickness and passing time. The film containing Shirazi thyme showed a clear antibacterial effect. The film can be described as a unique chitosan film, a moisture-absorbing antibacterial pad, and a new idea for active food packaging to increase the shelf life of foods with fully degradable properties.

Acknowledgements

The financial support was provided by Shiraz University, Iran. The Agricultural Research Education and Extension Organization (AREEO), the Animal Science Research Institute (ASRI), and the Agricultural Engineering Research Institute (AERI), Iran, are truly acknowledged.

Conflict of interest

The authors declare that they have no conflicts of interest.

References

Adams, RP and Sparkman, OD (2007). Review of identification of essential oil components by gas chromatography/mass spectrometry. J. Am. Soc. Mass Spectrom., 18: 803-806.

Amidi, M; Mastrobattista, E; Jiskoot, W and Hennink, WE (2010). Chitosan-based delivery systems for protein therapeutics and antigens. Adv. Drug. Deliv. Rev., 62: 59-82.

Amjadi, S; Emaminia, S; Davudian, SH; Pourmohammad, S; Hamishehkar, H and Roufegarinejad, L (2019). Preparation and characterization of gelatin-based nanocomposite containing chitosan nanofiber and ZnO nanoparticles. Carbohydr. Polym., 216: 376-384. doi.org/10.1016/j.carbpol.2019.03.062.

ASTM International (2007). Standard test methods for tensile properties of thin plastic sheeting. D882-02. Annual book of ASTM Standards. 14.02. United States.

Bhardwaj, A; Alam, T and Talwar, N (2019). Recent advances in active packaging of agri-food products: a review. J. Postharvest Technol., 07: 33-62.

Cao, X; Chen, Y; Chang, PR; Stumborg, M and Huneault, MA (2008). Green composites reinforced with hemp nanocrystals in plasticized starch. J. Appl. Polym. Sci., 109: 3804-3810.

Chaichi, M; Hashemi, M; Badii, F and Mohammadi, A (2017). Preparation and characterization of a novel bio nanocomposite edible film based on pectin and crystalline nanocellulose. Carbohydr. Polym., 157: 167-175.

Chanphai, P and Tajmir-Riahi, HA (2018). Conjugation of tea catechins with chitosan nanoparticles. Food Hydrocoll., 84: 561-570.

FICCI (Federation of Indian Chambers of Commerce and Industry) (2016). A report on plastics industry. In: Proceedings of the 2nd National Conference on Plastic Packaging-the Sustainable Choice, New Delhi.

Frone, AN; Berlioz, S; Chailan, JF and Panaitescu, DM (2013). Morphology and thermal properties of PLA-cellulose nanofibers composites. Carbohydr. Polym., 91: 377-384.

Jalaei, J; Fazeli, M; Rajaian, H and Shekarforoush, SS (2014). *In vitro* antibacterial effect of wasp (*Vespa orientalis*) venom. J. Venom. Anim. Toxins Incl. Trop. Dis., 20: 1-6. doi: 10.1186/1678-9199-20-22.

Jeevahan, J and Chandrasekaran, M (2019). Nanoedible films for food packaging: a review. J. Mater Sci., 54: 12290-12318.

Kanagaraj, S; Varanda, FR; Zhiltsova, TV; Oliveira, MS and Simoes, JAO (2007). Mechanical properties of high-density polyethylene/carbon nanotube composites. Compos. Sci. Technol., 67: 3071-3077.

Koo, JH (2019). Polymer nanocomposites: Processing, characterization, and applications. 2nd Edn., New York, McGraw-Hill Education. P: 272.

Kumar, MNVR (2000). A review of chitin and chitosan applications. React. Funct. Polym., 46: 1-27.

Lavorgna, M; Piscitelli, F; Mangiacapra, P and Buonocore, GG (2010). Study of the combined effect of both clay and glycerol plasticizer on the properties of chitosan films. Carbohyd. Polym., 82: 291-298.

Ma, X; Chang, PR; Yang, J and Yu, J (2009). Preparation and properties of glycerol plasticized-pea starch/zinc oxide-starch bionanocomposites. Carbohyd. Polym., 75: 472-478.

Ma, J; Zhu, W; Tian, Y and Wang, Z (2016). Preparation of zinc oxide-starch nanocomposite and its application on coating. Nanoscale Res. Lett., 11: 1-9. Doi: 10.1186/s11671-016-1404-y.

Mandal, A and Chakrabarty, D (2015). Characterization of nanocellulose reinforced semi-interpenetrating polymer network of poly (vinyl alcohol) and polyacrylamide composite films. Carbohyd. Polym., 134: 240-250.

Mohamad, NA and Fahmy, MM (2012). Synthesis and antimicrobial activity of some novel cross-linked chitosan hydrogels. Int. J. Mol. Sci., 13: 11194-11209.

Morales-González, JA; Madrigal-Bujaidar, E; Sánchez-Gutiérrez, M; Izquierdo-Vega, JA; Valadez-Vega, MC; Álvarez-González, I; Morales-González, A and Madrigal-Santillán, E (2019). Garlic (*Allium sativum*): A brief review of its antigenotoxic effects. Foods. 8: 343. doi: 10.3390/foods8080343.

Noorbakhsh-Soltani, SM; Zerafat, MM and Sabbaghi, S (2018). A comparative study of gelatin and starch-based nano-composite films modified by nano-cellulose and chitosan for food packaging applications. Carbohyd. Polym., 189: 48-55. doi.org/10.1016/j.carbpol.2018.02.012.

Ozdemir, M and Floros, JD (2004). Active food packaging technologies. Criti. Rev. Food Nutr., 44: 185-193.

Qin, Y; Liu, Y; Yuan, L; Yong, H and Liu, J (2019). Preparation and characterization of antioxidant, antimicrobial and pH-sensitive films based on chitosan, silver nanoparticles and purple corn extract. Food Hydrocoll., 96: 102-111.

Radusin, T; Ristić, IS; Pilić, BM and Novaković, AR (2016). Antimicrobial nanomaterials for food packaging applications. Food Feed Res., 43: 119-126.

Rahimi, R; ValizadehKaji, B; Khadivi, A and Shahrjerdi, I (2019). Effect of chitosan and thymol essential oil on quality maintenance and shelf-life extension of peach fruits cv. 'Zaferani'. J. Hortic. Postharvest Res., 2: 143-156.

Rattanachaikunsopon, P and Phumkhachorn, P (2009). Shallot (*Allium ascalonicum* L.) oil: Diallyl sulfide content and antimicrobial activity against food-borne pathogenic bacteria. Afr. J. Microbiol. Res., 3: 747-750.

Ribeiro, MC; Correa, VLR; da Silva, FKL; de Oliveira Neto, JR; Casas, AA; de Menezes, LB and Amara, AC (2018). Improving peptide quantification in chitosan nanoparticles. Int. J. Biol. Macromol., 119: 32-36.

SAS (2013). Proprietary Software Version 9.00. SAS Institute: Cary, NC, USA.

Schiffman, JD and Schauer, CL (2007). One-stepelectrospinning of crosslinked chitosan fibers. Biomacromolecules. 8: 2665-2667.

Seydim, AC and Sarikus, G (2006). Antimicrobial activity of whey protein based edible films incorporated with oregano, rosemary and garlic essential oils. Food Res. Int., 39: 639-644.

Shirdel, M; Tajik, H and Moradi, M (2017). Combined activity of colloid nanosilver and *Zataria nultiflora* Boiss essential oil mechanism of action and biofilm removal activity. Adv. Pharm. Bull., 7: 621-628.

Silva, F; Domingues, FC and Nerín, C (2018). Control microbial growth on fresh chicken meat using pinosylvin inclusion complexes-based packaging absorbent pads. LWT-Food Sci. Technol., 89: 148-154.

Sun, X; Jia, P; Zhe, T; Bu, T; Liu, Y; Wang, Q and Wang, L (2019). Construction and multifunctionalization of chitosan-based three-phase nano-delivery system. Food Hydrocoll., 96: 402-411.

Turalija, M; Bischof, S; Budimir, A and Gaan, S (2016). Antimicrobial PLA films from environment friendly additives. Compos. B. Eng., 102: 94-99.

van der Lubben, IM; Verhoef, JC; Borchard, G and Junginger, HE (2001). Chitosan and its derivatives in mucosal drug and vaccine delivery. Eur. J. Pharm. Sci., 14: 201-207.

Vigneshwaran, N; Kumar, S and Kathe, AA (2006). Functional finishing of cotton fabrics using zinc oxide-soluble starch nanocomposites. Nanotechnology. 17: 5087-5095.

Wei, D; Sun, W; Qian, W; Ye, Y and Ma, X (2009). The synthesis of chitosan-based silver nanoparticles and their antibacterial activity. Carbohydr. Res., 344: 2375-2382.

WU, N; ZU, YG and WANG, W (2008). Antimicrobial activities of garlic essential oil. Food Sci., 3: 103-105.

Yang, YN; Lu, KY; Wang, P; Ho, YC; Tsai, ML and Mi, FL (2020). Development of bacterial cellulose/chitin multi-nanofibers based smart films containing natural active microspheres and nanoparticles formed in situ. Carbohydr. Polym., 228: 115370. doi.org/10.1016/j.carbpol.2019.115370.

Yin, MC and Cheng, WS (2003). Antioxidant and antimicrobial effects of four garlic-derived organosulfur compounds in ground beef. Meat Sci., 63: 23-28.